

Journal of
Mechanics of
Materials and Structures

**DESIGN OF CRACK-RESISTANT TWO-DIMENSIONAL PERIODIC
CELLULAR MATERIALS**

Fabian Lipperman, Michael Ryvkin and Moshe B. Fuchs

Volume 4, N° 3

March 2009



mathematical sciences publishers

DESIGN OF CRACK-RESISTANT TWO-DIMENSIONAL PERIODIC CELLULAR MATERIALS

FABIAN LIPPERMAN, MICHAEL RYVKIN AND MOSHE B. FUCHS

The resistance to macrocrack propagation in two-dimensional periodic cellular materials subjected to uniaxial remote stresses is improved by redistributing the material of the solid phase. The materials are represented by beam lattices with regular triangular or hexagonal patterns. The purpose of the design is to minimize the maximum tensile stress for all possible crack locations allowed by the material microstructure. Two design cases are considered. In the cell design case material is redistributed between the otherwise uniform elements of the repetitive cell. In the element design case the shape of identical elements is optimized. The analysis of such infinite trellis with an arbitrary macroscopic crack is enabled by an efficient exact structural analysis approach. It is shown that the fracture toughness of the triangular layout can be significantly increased by redistribution of the material between the elements with uniform cross sections while for the case of hexagonal lattice the effect is achieved mainly by using identical elements with variable thickness distribution.

1. Introduction

The present paper is concerned with the improvement of the resistance of periodic cellular materials to the propagation of mature cracks by redesigning the repetitive cell. The two-dimensional cellular materials, or honeycombs, considered here are modeled as lattices with rigidly connected beam elements exhibiting both axial and flexural stiffness. Borrowing from the continuous case the resistance to crack propagation of a cellular material is given by the fracture toughness K_C . In contrast to a continuous material where the fracture toughness is determined experimentally, in cellular materials, where the tip of a macroscopic crack can be always associated with a void, thus precluding singularities in the stress field, the fracture toughness can, in principle, be determined numerically in terms of the rupture stress of the parent brittle material. The aim of the present paper is to improve the fracture toughness of cellular material by redesigning the repetitive cell using a formal mathematical programming approach.

A numerical structural optimization process is basically a conjunction of an analysis module embedded within an optimization algorithm. The availability of an efficient and robust analysis tool is thus a central concern since the optimizer will usually navigate through a plethora of candidate designs, each requiring a separate analysis, before reaching the best configuration. We need therefore an adequate capability for a detailed analysis of a cellular material in a given stress field in the presence of a crack. The basic problem in the presence of a crack is that the periodicity of the structure is lost, which causes difficulties for the analysis. Some authors have obtained the fracture toughness of cellular material numerically, most of them in some restrictive cases. The published methods of determining the fracture toughness either

Keywords: fracture toughness, honeycombs, design, discrete Fourier transform.

The second author gratefully acknowledges the support of the ISF (Israel Science Foundation) under grant No. 838/06.

involve some sort of representation of the honeycomb as an equivalent continuum (homogenization) — an indirect approach — as in [Maiti et al. 1984; Gibson and Ashby 1997; Chen et al. 1998], or tackle the problem directly with a finite element method by reducing the infinite honeycomb to a finite-size model [Huang and Gibson 1991; Schmidt and Fleck 2001; Choi and Sankar 2005; Fleck and Qiu 2007; Quintana Alonso and Fleck 2007].

In all these examples, and to the best of our knowledge, also among other publications which deal with the fracture toughness estimation of cellular materials no numerical work was published on the fracture toughness of honeycombs with asymmetric or irregular topologies. Recently, a general approach which uses exact structural analysis for a crack in an infinite lattice was presented in [Lipperman et al. 2007a] to determine the fracture toughness of honeycombs with prismatic-like elements. The method can accommodate any topology of the unit repetitive cell, with or without symmetry, and any type of remote loading.

The above references deal with the determination of the fracture toughness of cellular material. The present paper intends to redesign the unit cell in order to improve the fracture toughness, that is, to improve the resistance of all mature cracks which may exist in the cellular material, to propagate when subjected to a uniaxial stress field in a given direction. Since cracks are assumed *ab initio*, all possible crack types and orientations compatible with the internal arrangement of the microstructure of the particular material are made allowance for in each case. To this respect, this is probably a first attempt for a systematic design of crack-resistant honeycombs (we use the term *crack-resistant* to indicate the resistance of mature cracks to propagate).

Two design formulations are presented starting with the *cell* design case where material is moved between the otherwise uniform elements of the unit cell. In the *element* design formulation all the elements of the unit cell are identical and the shape of a typical prismatic element of variable cross-section is optimized. Note, elements with variable thickness were considered in [Warren and Kraynik 1987], where the linear elastic response of an *undamaged* hexagonal honeycomb was studied for three different element shapes, and in [Warren and Kraynik 1988] for a tetrahedral unit cell, but the shape of the elements were not optimized. The present paper deals with two basic topologies: regular triangular and regular hexagonal lattices. As indicated the honeycombs considered here will be redesigned to resist crack propagation of any possible mature crack under a given unidirectional remote tensile loading.

For the analysis, the method in [Lipperman et al. 2007a] is used. The analysis is direct, in the sense that it remains in the discrete realm without first associating the honeycomb with a continuous material using homogenization. A conjunction of the structural variation method of Majid et al. [1978], the representative cell method of Nuller and Ryvkin [1980] and stress localization [Michel et al. 1999; Lipperman et al. 2008a] allows for an exact analysis of fractured honeycombs with repeating unit cells of any shape and subjected to any type of remote loading. With this versatile analysis module at hand the honeycombs are optimized for maximum resistance to crack propagation.

In Section 2 the design problem is formulated. Section 3 gives a succinct description of the analysis process. In Sections 4 and 5 we present the redesign of the honeycombs for best crack-resistance. The paper closes with a summary of the main results and some conclusions (Section 6).

2. The design formulations

The purpose of the design is to produce honeycombs which have improved resistance to crack propagation under remote stresses. This property is characterized by the honeycomb fracture toughness. Huang and Gibson [1991], who evaluated the stress field in the vicinity of a Mode I crack of length $2a$ in a square-celled honeycomb, calculated this quantity by means of the formula

$$K_C = \sigma_r \sqrt{\pi a}, \quad (1)$$

where σ_r is the remote tensile loading corresponding to the onset of fracture, that is, when the most stressed element in the crack-tip vicinity fails. We will follow this approach completed by the assumption that noninteracting cracks of same length, of all possible types and orientations, dictated by the material microstructure, are present simultaneously. Consequently, the magnitude of σ_r in (1) is defined by the stress field in the vicinity of the most dangerous crack. Clearly, the crack length used in the simulations must be large enough such as to produce self-similar K -fields close to the crack tips. The issue of possible crack types was investigated by Lipperman et al. [2007b], who found numerically that they are parallel to the microstructure symmetry planes. It should be noted that the optimization of the fracture properties was carried out for a specific loading direction.

The redesign is performed on honeycombs with two popular patterns: equilateral triangles and regular hexagons (Figure 1). The unit cells of the planar repetitive structures have walls of length L , rectangular cross sections of thickness t and a unity inward depth. For the analysis model, the cell walls are represented by rigidly connected Euler–Bernoulli beam elements, including their axial rigidity. A displacement-based analysis is used with 3 degrees of freedom defined at each node. The bulk material is assumed isotropic, homogeneous, linear-elastic and brittle with a rupture modulus σ_{fs} . The honeycombs are subjected to a uniaxial remote stress σ_r as shown in Figure 1.

We will take into account all the possible straight paths which can be formed by the sequential fracture of elements along the lattice axes of symmetry. As shown in Figure 2, top, the triangular pattern has a single crack type, denoted by T1, whereas the hexagonal grid exhibits 3 crack types: H1, H2 and H3 (see Figure 2, bottom). It will be seen that the macroscopic cracks in Figure 2 can for both patterns be rotated three times by an angle of $\pi/3$ radians, yielding three possible propagation orientations in each case. Consequently, the triangular layout has in total 3 possible cracks whereas the hexagonal lattice has 9 possible cracks.

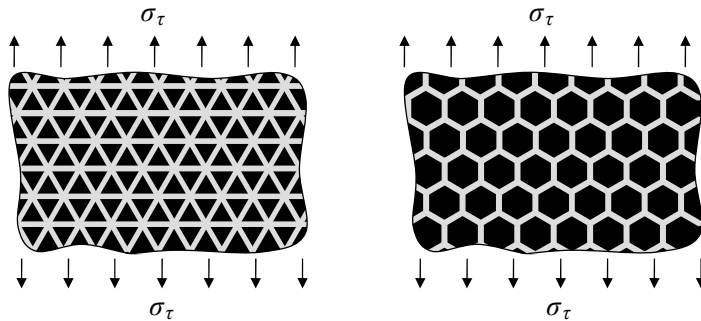


Figure 1. Honeycombs with equilateral triangles (left) and regular hexagons (right), subjected to a uniaxial remote loading.

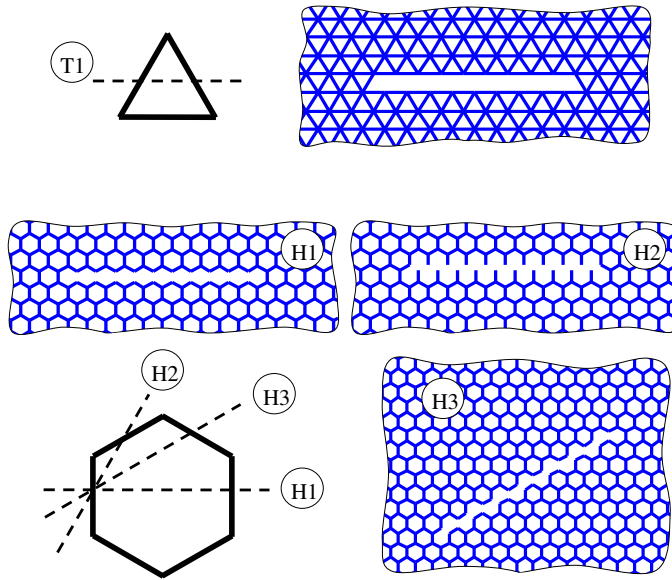


Figure 2. The possible macrocrack paths types of the triangular and hexagonal, honeycombs.

We consider two design cases. In the *cell design* case the beam-elements of the unit cell are uniform and the design variables are the thicknesses of the elements (Figure 3, left). During the optimization process material is moved between the elements until the optimal layout is reached. Moving material between elements creates nonsymmetric unit cells and as stated earlier, there are no published results for the analysis of such materials, with or without cracks. In the *element design* case the unit cells are composed of an identical typical element of variable thickness (Figure 3, right). The optimization searches for the optimal shape of the typical element and the design variables are parameters which govern the contour of the element.

A crack propagates by the failure of an element in the crack tip vicinity. It is assumed that an element will fail when the tensile stress, anywhere along the element, reaches the rupture modulus or when the axial load in a compressed element reaches the Euler buckling load. Note that the maximal tensile stress in a uniform element (cell design case, shown on the left in Figure 3) will occur at one of the ends of

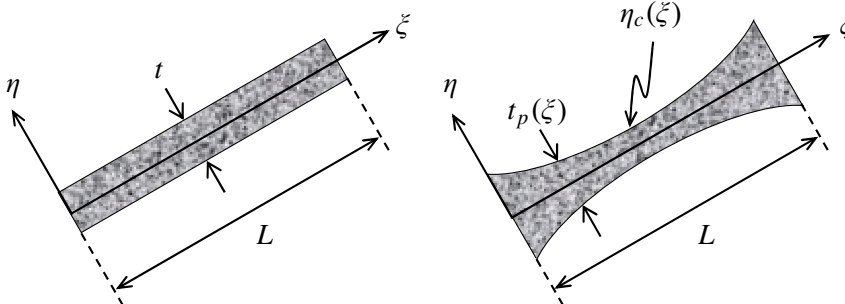


Figure 3. Beam elements with uniform and variable cross-sections.

the element. On the other hand, with variable cross-sections (element design case, shown on the right in Figure 3), the maximum stress can also occur at intermediate locations. As indicated, we can have several possible crack types and crack orientations. Consequently, we are in the presence of a minimax problem in the sense that we want to minimize the maximum stress anywhere along elements in the front of any possible crack and thus improving the resistance of the structure to the propagation of existing cracks. Minimizing the maximum stress in the elements is commensurate with maximizing the allowable remote stress, that is, maximizing K_C .

3. Analysis considerations

A central ingredient in a structural optimization scheme is the analysis module which provides the internal forces in the structure for any given candidate design. In the present case we need to analyze a fractured cellular material under remote uniaxial tension. The crack is formed by a series of fractured elements in contiguous cells along a linear path. It must be sufficiently long, so that the K -field in its vicinity emerges, allowing one to determine the fracture toughness. Since the fractured elements do not contribute to the stiffness of the assembly they can be removed from the analysis model which results in an infinite structure which is no longer periodic subjected to uniaxial tension at infinity. The central idea in analyzing the cracked honeycomb is to consider the failed elements as a finite set of components whose stiffness was modified (in our case, reduced to zero) in an otherwise repetitive infinite structure. We will refer to the undamaged honeycomb as the *nominal* structure, the cracked honeycomb as the *modified* structure and the stresses at infinity will be the *nominal loads*. The analysis will be based on the structural variations method of Majid et al. [1978], which is an efficient reanalysis method when only part of the stiffnesses of a structure are modified. In particular, for the broken elements considered here, the modification is to set the stiffnesses to zero. This method determines the internal forces in the modified structure on the basis of analyses performed on the nominal structure under the nominal loads and under self-equilibrating loads. The latter are unit and opposite forces applied in turn to the extremities of the elements that will eventually be removed to form the crack (Figure 4). This method suits the present needs perfectly since we need to analyze only intact infinite repetitive structures.

For the analysis of the nominal structure under the nominal loads, that is, the uniaxial stress field, we follow the methodology for stress localization for honeycombs in a macroscopic stress field [Michel et al. 1999]. Stress localization gives the detailed stresses in the repetitive cell of a cellular material subjected

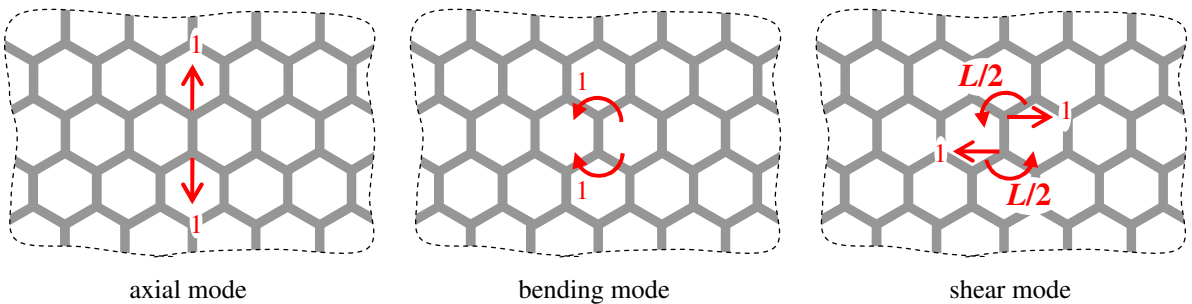


Figure 4. The unit loads applied at the nodes of an arbitrary rigid-jointed element of the hexagons honeycomb.

to a periodic stress field, without the need for prior homogenization. We will be using a slightly modified version of stress localization developed in [Lipperman et al. 2008a].

The unit loads solutions are obtained by the representative cell method [Nuller and Ryvkin 1980; Ryvkin and Nuller 1997], which enables to solve infinite and repetitive structures subjected to arbitrary loads, as opposed to periodic loads (see, for instance, [Ryvkin et al. 1999; Fuchs and Ryvkin 2002; Fuchs et al. 2004]). A discrete Fourier transform replaces the problem formulated for an infinite structure by an equivalent problem defined over the repetitive cell, albeit in transformed variables. After solving the analysis equations in the transformed space, inverse transforms can produce the requested analysis information in any cell of the infinite structure. It is instructive to emphasize that both stress localization and the representative cell method perform the analysis on a single repetitive module.

4. Optimal design of the unit cell

In the cell design example we maximize the fracture toughness K_C of the cellular material by redistributing the material between the uniform elements of the unit cell while maintaining a constant material density. This is akin to minimizing the maximum skin stress in elements in the vicinity of the crack tips for all possible crack types and orientations. The mathematical programming formulation of this min-max optimization problem is

$$\min_t \max \{ \boldsymbol{\sigma}(t) \text{ such that } \rho(t) = \rho_r \}, \quad (2)$$

where t is the design vector composed of the unit cell elements thicknesses, $\boldsymbol{\sigma}(t)$ is the vector containing the set of largest stresses in elements that are to be considered for all possible cracks, $\rho(t)$ is the relative density of the cellular material defined as the ratio of the density of the honeycomb over the density of the bulk material and ρ_r is a given relative density, taken here as $\rho_r = 0.15$. The cracks length $2a$ is chosen sufficiently long to ensure continuum fracture mechanics behavior characterized by the proportionality of the near tip stress field to the square root of the crack length.

Failure of an element is assumed to occur when the normal stress anywhere along the element reaches the critical tension stress or the critical compression stress. The critical tension stress σ_{cr}^T is simply the bulk material rupture modulus σ_{fs}

$$\sigma_{cr}^T \equiv \sigma_{fs} \quad (3)$$

and the critical compression stress is adopted as the Euler buckling stress for the uniform hinge supported element

$$\sigma_{cr}^B \equiv \frac{E}{12} \pi^2 (t/L)^2, \quad (4)$$

where E is the Young's modulus of the solid material and t is the thickness of the element. Hinge supports are assumed for conservative reasons. In order to set the tensional and buckling modes on a common footing we have assumed $E/\sigma_{fs} = 10^3$, which is a common ratio for ceramics and many metal materials [Bolton 1998]. Consequently

$$\frac{\sigma_{cr}^T}{\sigma_{cr}^B} = \frac{12}{10^3 \pi^2 (t/L)^2}. \quad (5)$$

The value σ_j of the stress vector σ is defined by the most critical axial stress failure mode

$$\sigma_j = \max(\sigma_j^T; \sigma_j^B), \tag{6}$$

where σ_j^T and σ_j^B are the skin stresses related to the tensional and buckling failure modes for element j , respectively given by

$$\sigma_j^T = \frac{N_j}{t_j} + \max\left(\frac{6|M_{1j}|}{t_j^2}; \frac{6|M_{2j}|}{t_j^2}\right) \quad \text{and} \quad \sigma_j^B = \frac{-N_j}{t_j} \left(\frac{\sigma_{cr}^T}{\sigma_{cr}^B}\right)_j. \tag{7}$$

N_j is the internal axial force in element j , and M_{1j}, M_{2j} are the internal bending moments at its extremities.

We consider two cell layouts, the triangular pattern and the hexagonal one. With each pattern we first take the basic repeating cell as the redesign unit. Next we consider a larger redesign unit consisting of four basic cells thus quadrupling the number of design variables and consequently enriching the optimization space. All computations were performed on a Matlab platform and for the actual minimization we have used the `fminimax` subroutine of Matlab which implements a sequential quadratic programming method.

4.1. Triangles: one basic unit. As a first design scenario we consider the triangular honeycomb for which the smallest repeating pattern possesses three elements, as shown in Figure 5(a). They will typically be referred to as 1-elements, 2-elements and 3-elements. The constraint on the relative density of the material is

$$\rho(t) \equiv \frac{2}{\sqrt{3}L} \sum_{i=1}^3 t_i = 0.15. \tag{8}$$

As mentioned, the triangle has only one crack type, T1, with 3 possible orientations yielding the macroscopic cracks $T1_0, T1_{\pi/3}, T1_{2\pi/3}$, where the orientation angles θ_p are given in the subscript. In parts (b) and (c) of Figure 5 one can see a depiction of cracks $T1_0$ and $T1_{\pi/3}$.

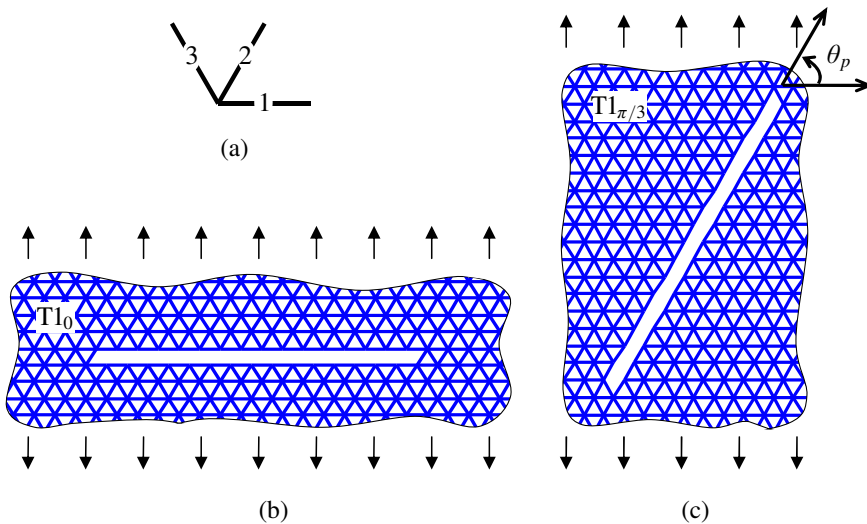


Figure 5. (a) The unit cell of the triangles honeycomb with (b) $\theta_p = 0$ and (c) $\theta_p = \pi/3$ paths orientations.

Each of the three cracks can end in front of two different unit cell elements. For instance, crack $T1_0$ in [Figure 5\(b\)](#) ends in front of a 2-element but it could also stop in front of a 3-element. For the triangular case (one basic unit) we need to ensure that none of the $3 \times 2 = 6$ possible cracks propagates while maximizing the fracture toughness. This triangular pattern with three design variables is a relatively simple case. We will see in the sequel that in more intricate designs with more elements in the repeating unit we may have several possible cracks in the material. It is therefore worthwhile to try to reduce the number of candidate cracks prior to solving (2). We need to determine not only which cracks should be considered for the optimization but also in front of which element they end.

The structure was analyzed in the initial configuration (identical elements) for every possible crack, and cracks with relatively low near-tip stresses were discarded. In the case of triangular cells this left only crack $T1_0$. Since we omit cracks on the basis of the initial design the optimal solution was again checked against all the cracks to ensure that in the final layout no crack propagates.

An arguably intrinsic feature of designing for crack-resistance is that including two cracks of a same type and orientation but with different end-elements may impede the process from reaching the optimal solution. To illustrate the concept consider again the $T1_0$ of the triangular pattern. It propagates by sequential breaking of 2- and 3-elements — with the labeling as in [Figure 5\(a\)](#) — along the crack line illustrated in [Figure 5\(b\)](#). Including both cracks in the optimization will yield a symmetric design with equal thicknesses for elements 2 and 3 (and half the thickness for element 1). Consequently, a $T1_0$ crack, whether facing a 2-element or a 3-element will not propagate. However, this may not be the best solution. In contrast to classical structural design where no failure is tolerated, with crack propagation we do not really care if a crack facing a 2-element breaks that element as long as it stops in front of the subsequent 3-element (or vice-versa.) We could thus weaken the 2-elements and reinforcing the 3-elements by moving material from 2 to 3. By setting the *trap* at 3 (or at 2) we should produce better resistant materials albeit with nonsymmetric repetitive cells. This can be achieved by including only one $T1_0$ crack, facing either a 2- or a 3-element, in the optimization formulation.

For the triangular case with 3 design variables we need to include only one crack. With unit cells of complex geometries and more design variables, the selection of cracks and corresponding traps is not always obvious and in such cases (2) must be solved separately for several alternatives.

In this example we selected 2 as the trap element and the optimization in (2) gave elements of thicknesses

$$t_1^{\text{opt}} = 0.026L, \quad t_2^{\text{opt}} = 0.053L, \quad t_3^{\text{opt}} = 0.051L \tag{9}$$

with a normalized fracture toughness

$$K_C^{T_3} / (\sigma_{fs} \sqrt{L}) = 0.091, \tag{10}$$

where the superscript indicates that we deal with a triangular layout with 3 design variables. The improvement of this design with respect to a design with equal thicknesses [[Lipperman et al. 2007a](#)] is

$$\frac{K_C^{T_3}}{K_C^T} = 1.20. \tag{11}$$

Thus, the thicknesses distribution obtained in (9), increases the K_C of the triangular honeycomb, loaded in the direction given in parts (b) and (c) of [Figure 5](#), by 20%.

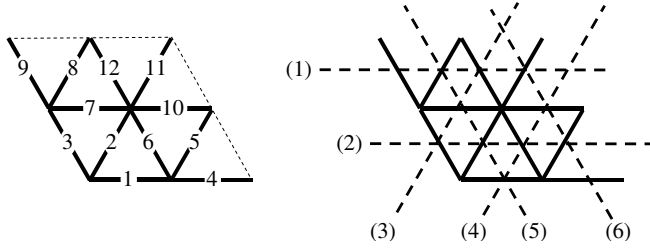


Figure 6. Left: The enlarged unit cell of the triangles honeycomb. Right: the six T1 propagation possibilities.

4.2. Triangles: four basic units. Improved results can be expected if we increase the size of the repeating cell and therefore the number of design variables. In this example we consider a repeating cell composed of 4 basic units. We have thus 12 design variables and 6 different T1 possibilities (Figure 6). However, as noted in Section 4.1, it suffices to consider the two horizontal paths. The relative density constraint is now

$$\rho(\mathbf{t}) \equiv \frac{1}{2\sqrt{3}L} \sum_{i=1}^{12} t_i = 0.15. \tag{12}$$

The selection of the trap elements is a little more intricate. Here one needs to make allowance for cracks to propagate in both directions. After due considerations the traps were set at elements 2, 6, 11 and 12 and from symmetry the number of independent design variables could be reduced to 4. The optimal layout given in Figure 7 has thicknesses

$$\begin{aligned} t_2^{\text{opt}} = t_6^{\text{opt}} = t_{11}^{\text{opt}} = t_{12}^{\text{opt}} &= 0.086L, & t_1^{\text{opt}} = t_4^{\text{opt}} &= 0.025L, \\ t_3^{\text{opt}} = t_5^{\text{opt}} = t_8^{\text{opt}} = t_9^{\text{opt}} &= 0.017L, & t_7^{\text{opt}} = t_{10}^{\text{opt}} &= 0.029L \end{aligned} \tag{13}$$

with an optimal fracture toughness $K_C^{T_{12}}/(\sigma_{fs}\sqrt{L}) = 0.110$ which gives an improvement with respect to the original design of

$$\frac{K_C^{T_{12}}}{K_C^T} = 1.45. \tag{14}$$

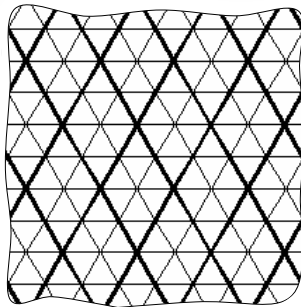


Figure 7. An option for an optimal triangles honeycomb where the maximal length and the minimal thickness of its elements have been previously set.

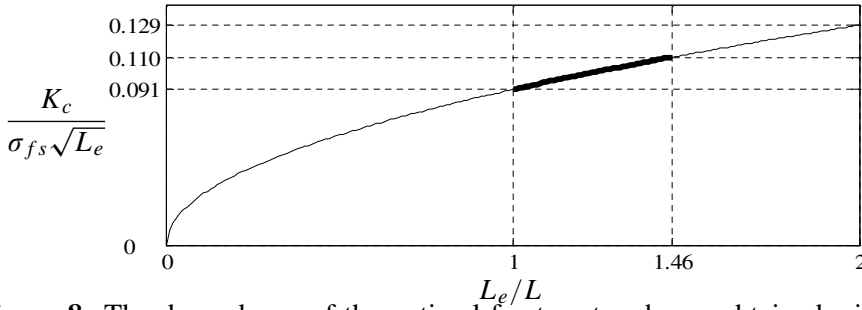


Figure 8. The dependence of the optimal fracture toughness obtained with 3 design variables on the scale length of the elements.

At this juncture it is instructive to address an issue related to the relative scale of the grid. In [Figure 8](#) we show the dependence of the optimal fracture toughness on the element length L_e where the relative density was kept unchanged by maintaining a constant value of t/L_e . We assume that the basic value $K_C^{T_3}/(\sigma_{fs}\sqrt{L}) = 0.091$ of (10) was obtained for a unit element length, that is, when $L_e/L = 1$. The fracture toughness is a square root function of the element length and doubling the latter ($L_e = 2L$) should produce $K_C^{T_3}/(\sigma_{fs}\sqrt{L}) = 0.091\sqrt{2} = 0.129$, as indicated on the figure. This result could have been obtained by the optimization in the absence of Euler buckling constraints by removing elements 5, 6, 7, 8, 10 and 12. This is a classical case of a disjoint design space. The double-sized triangle lies in the shadow of the buckling constraints, however, once it is reached, the design is acceptable because the buckling constraints on the now vanished elements are no longer valid. The optimal design of the present problem should in fact be the trivial solution in the form of a triangle with double lengths and thicknesses.

We can however make a case for the design in [Figure 7](#). Clearly, increasing L_e will improve the fracture toughness but it also increases the size of the *holes* or apertures in the material. The *holes* in the triangles with $L_e = 2L$ have doubled and if we want to limit the size of the holes to the scale $L_e = L$ (think of a net capturing fish) the design in [Figure 7](#) is to be preferred. In fact, as shown on the graph, the design in [Figure 7](#) of scale $L_e = L$ is equivalent to an optimal solution with 3 design variables of scale $L_e = 1.46L$.

4.3. Hexagons: one basic unit. The basic hexagonal pattern has three design variables, with a relative density constraint

$$\rho(\mathbf{t}) \equiv \frac{2}{3\sqrt{3}L} \sum_{i=1}^3 t_i = 0.15. \tag{15}$$

As noted from [Figure 2](#), right, there are a total of 9 propagation paths: $H1_{0,\pi/3,2\pi/3}$, $H2_{0,\pi/3,2\pi/3}$, $H3_{\pi/6,\pi/2,5\pi/6}$. A preliminary investigation of the initial design (equal thicknesses) has shown that the problem could be simplified. Because of symmetry, as noted for instance in [Figure 9](#) for the $H1_0$ crack, we have $t_2 = t_3$ and the set of cracks can be reduced to $H1_0$, $H2_0$ and $H3_{\pi/6}$ in view of the fact that the constraints produced by the remaining cracks can be shown to be nonactive.

The optimum result is

$$t_1^{\text{opt}} = 0.119L \quad \text{and} \quad t_2^{\text{opt}} = t_3^{\text{opt}} = 0.135L \tag{16}$$

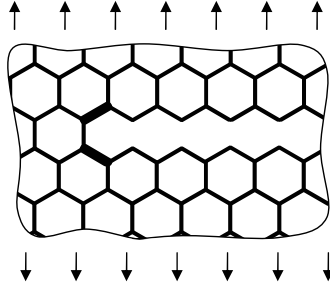


Figure 9. The H_{10} macrocrack with its two most loaded elements (in bold).

for $K_C^{H_3}/(\sigma_{fs}\sqrt{L}) = 0.016$, an improvement of only 6% over the fracture toughness with equal cross-sections (0.015), given in [Lipperman et al. 2007a]. The resistance to macrocrack propagation in this case is only moderately improved.

The location of the most loaded elements (Figure 9) may be counterintuitive however an earlier work on crack nucleation and propagation has shown that this type of crack under same loads at some early stage of the crack formation changed direction from the path perpendicular to the loading to a direction inclined by 60° [Lipperman et al. 2007b]. The most loaded elements at the crack-tip are probably the harbingers of the kink in the crack path.

4.4. Hexagons: four basic units. We now consider an augmented design domain, composed of four basic unit cells with 12 design variables, as shown in Figure 10. The relative density constraint here is

$$\rho(\mathbf{t}) \equiv \frac{1}{6\sqrt{3}L} \sum_{i=1}^{12} t_i = 0.15. \tag{17}$$

The number of design variables could be reduced from 12 to 5 and from the 18 possible propagation paths only 5 were retained.

The thickness distribution for the optimal solution is

$$\begin{aligned} t_7^{\text{opt}} &= 0.15L, & t_{10}^{\text{opt}} &= 0.01L, & t_2^{\text{opt}} &= t_6^{\text{opt}} = t_{11}^{\text{opt}} = t_{12}^{\text{opt}} = 0.09L, \\ t_1^{\text{opt}} &= t_4^{\text{opt}} = 0.15L, & t_3^{\text{opt}} &= t_5^{\text{opt}} = t_8^{\text{opt}} = t_9^{\text{opt}} = 0.18L. \end{aligned} \tag{18}$$

A typical unit cell and an overview of the hexagonal pattern are depicted in Figure 11. In the optimal layout we notice ellipse-like quasiholes in the form of cells with embedded slender elements oriented along the remote stress direction. The optimal fracture toughness is here $K_C^{H_{12}}/(\sigma_{fs}\sqrt{L}) = 0.018$ which represents an increase of 18% over the initial design.

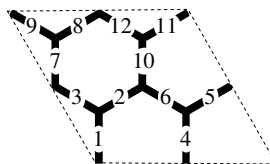


Figure 10. The enlarged hexagon unit cell with 12 elements.

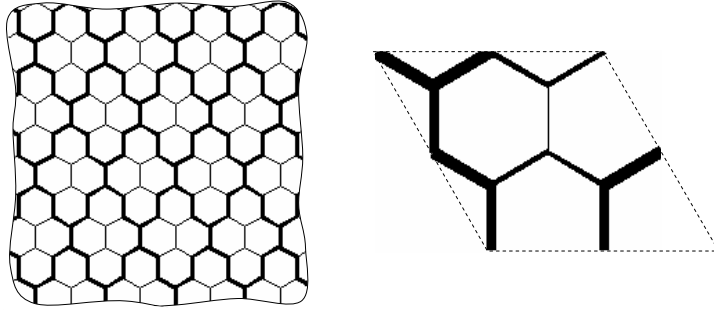


Figure 11. The optimal hexagonal honeycomb (left) with enlarged unit cell (right).

Unlike with the enlarged repetitive cell of the triangular honeycomb, the optimal hexagonal layout of scale L cannot be replicated on the present grid with elements of twice the length and thickness. The optimal design in [Figure 11](#) is thus the only possible layout.

4.5. Summary of results. The main results for the optimal design of the cellular material with relative density $\rho_r = 0.15$ are summarized in [Table 1](#) for both layouts. The fundamental difference between the two patterns is already apparent in the initial design. The triangular patterns are markedly more resistant to crack propagation than the hexagonal ones. This is to be attributed to the axial mode being dominant in triangular lattices whereas hexagons deform primarily in bending [[Deshpande et al. 2001](#)]. In addition, the optimization is relatively more effective for triangles, where, for instance, a 45% improvement was obtained for repetitive cells with 12 design variables as compared to 18% in the hexagonal case. The counterexamples in the next section will show that using elements of varying thickness will prove much more effective for bending dominated patterns than for materials where the axial mode is predominant.

	Triangles	Hexagons
Initial (equal thicknesses)	0.076	0.015
Optimized (3 design variables)	0.091 (20%)	0.016 (6%)
Optimized (12 design variables)	0.110 (45%)	0.018 (18%)

Table 1. Optimal fracture toughness $K_C/(\sigma_{fs}\sqrt{L})$ for triangular and hexagonal patterns with $\rho_r = 0.15$ for two sizes of the repetitive module. The initial values correspond to equal thickness elements. σ_{fs} is the rupture stress of the bulk material and L is the beams length. Improvements with respect to the initial design are given in parentheses.

5. Optimal design of the element

In this section we improve the material’s resistance to macroscopic crack propagation by using same beams but of variable thickness for the elements of the honeycomb. We assume the thickness of the elements $t_p(\xi)$ along $\xi = 0 \div L/2$ (see [Section 2](#)) to be

$$t_p(\xi) = 2\eta_c(\xi) = 2 \sum_{j=0}^p c_j \xi^j, \tag{19}$$

where p is the order of the polynomial and c_j are the parameters which define the shape of the elements and constitute the variables in this design problem. In addition we impose, for sound engineering design, a zero slope at the center of the symmetric element and positiveness of the thickness:

$$\frac{dt_p(\xi)}{d\xi} = 0 \quad \text{for } \xi = L/2, \quad t_p(\xi) \geq \varepsilon \quad \text{for } 0 \leq \xi \leq L/2, \tag{20}$$

with $\varepsilon = 10^{-5}L$. The mathematical programming formulation, solved with the same analysis and design subroutines as in Section 4, is here

$$\min_c \max \{ \boldsymbol{\sigma}(\mathbf{c}) \text{ such that } \rho(\mathbf{c}) = \rho_r \}, \tag{21}$$

where the design vector \mathbf{c} holds the coefficients c_j ($j = 0, 1, \dots, p$) of the polynomial. In line with (2), $\boldsymbol{\sigma}(\mathbf{c})$ is the vector containing the set of stresses that are to be considered for all possible cracks. The relative density constraint is now

$$\rho(\mathbf{c}) \equiv \frac{n_{ce}A_e}{A_{uc}} = \rho_r, \tag{22}$$

where n_{ce} ($= 3$ herein) is the number of elements of the unit cell, A_{uc} is the area of the unit cell and A_e is the area of the projection of the elements given by

$$A_e = 4 \int_0^{L/2} (c_0 + c_1\xi + \dots + c_p\xi^p) d\xi = 4 \sum_{j=0}^p \frac{c_j(L/2)^{j+1}}{j+1}. \tag{23}$$

For calculating the stiffness matrix of the beam element we have approximated the thickness by a piecewise linear function.

The material with the triangular pattern has a unit cell of area $A_{uc} = \sqrt{3}L/2$ and making allowance for the symmetry of the problem we considered only macroscopic cracks $T1_0$ and $T1_{\pi/3}$ (Figure 5). The optimal solution $t_p^{\text{opt}}(\xi)$ obtained with a second- and a third-order polynomial contour functions are presented in Table 2. The linear case is not addressed since it can not yield a zero slope at the middle of the element. Taking for baseline the material composed of elements with constant uniform cross-sections the improvement of the fracture toughness for honeycombs with optimized contours is given under the heading $K_C^{T_{\text{opt}}}$ in Table 2. It will be seen that the improvements are not dramatic. Better results were obtained for the triangle when transferring material between the elements of the unit cell design.

We now turn our attention to the hexagonal pattern ($A_{uc} = 3\sqrt{3}L/2$) where it was noticed that it suffices to include macroscopic cracks $H1_0$, $H2_0$ and $H3_{\pi/6}$, only. The results given in Table 3 clearly indicate a marked improvement in $K_C^{H_{\text{opt}}}$. In Figure 12 we have drawn the contours of the elements for different orders of the polynomial. It should be emphasized that the optimum was obtained for equal values of the skin stress at the root of an element and at mid-field. The latter could be calculated with

p	Contour function $t_p^{\text{opt}}(\xi)[10^{-2}L]$	$K_C^{T_{\text{opt}}}[\%]$
2	$4.6 - 1.4(\xi/L) + 1.4(\xi/L)^2$	4.2
3	$4.6 - 0.6(\xi/L) - 2.0(\xi/L)^2 + 3.4(\xi/L)^3$	4.8

Table 2. The optimal contour functions and fracture toughness increase of the triangles honeycomb.

p	Contour function $t_p^{\text{opt}}(\xi)[L]$	$K_C^{H_{\text{opt}}}$ [%]
2	$0.20 - 0.39(\xi/L) + 0.39(\xi/L)^2$	77.7
3	$0.17 - 0.05(\xi/L) - 0.82(\xi/L)^2 + 1.16(\xi/L)^3$	96.8
4	$0.18 - 0.15(\xi/L) + 0.13(\xi/L)^2 - 1.63(\xi/L)^3 + 2.50(\xi/L)^4$	103.7

Table 3. The optimal contour functions and fracture toughness increase of the hexagons honeycomb.

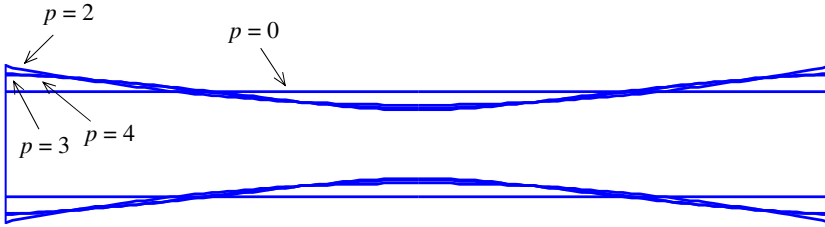


Figure 12. The optimal contours of the elements with $\rho_r = 0.15$.

relative confidence however at the root we have a concentration of material and consequently the model is locally less representative. As a consequence the stresses calculated at the ends may carry an error and should be utilized with care. The general trend is however clear and substantial improvements are to be gained by using variable thickness elements. In Figure 13 we give the shape of the hexagons obtained with optimal elements for densities $\rho_r = 0.15, 0.25$. The shape for the 0.25 density was added to show a tendency to form circular holes as the relative density of the cellular material increases. This

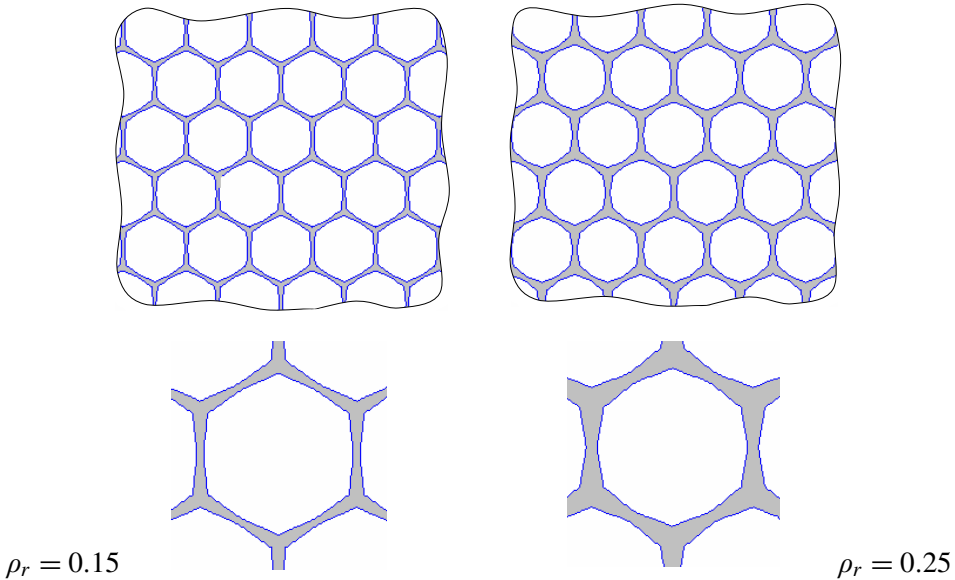


Figure 13. The topologies of the hexagons with the optimal elements obtained with the fourth-order contours, for $\rho_r = 0.15$ and $\rho_r = 0.25$.

corroborates a result obtained in a separate work on the K_{IC} fracture toughness of perforated plates where a parametric study on the optimal shape of holes has shown that for holes stacked in a hexagonal pattern, circular holes produced optimal designs [Lipperman et al. 2008b].

It is interesting to notice that variable thickness elements have a rather marginal effect on the fracture of the triangular pattern but are of paramount importance in hexagonal honeycombs. This feature is to be related to the flexion versus stretch dominance of the two families of cellular materials which were studied in this work.

6. Conclusions

This paper has presented a methodology for designing two-dimensional cellular materials with improved resistance to crack propagation under macroscopic uniaxial tensile stresses. The material is modeled as repetitive patterns of bending resistant elements and crack propagation by the sequential breaking of the, assumed, brittle beam elements. With such grids the material can have cracks in a limited number of directions and we have defined the fracture toughness concept which is akin to the fracture toughness generalized by assuming the presence of all possible noninteracting cracks. The purpose is to maximize the fracture toughness by redistributing the material in the repetitive cell in an optimal fashion. Both the analysis and design are confined to the repetitive unit. For the analysis of the material with a crack we have used the representative cell method in conjunction with stress localization. These methods produce the results for the cracked medium by analyzing infinite pristine structures. The analysis is thus exact within the realm of Bernoulli–Euler beams. Two types of honeycombs were studied. A stretch dominated material with triangular patterns and a material with hexagonal unit cells which exhibits substantial flexion. It was shown that the material with triangles has only one type of crack which can appear in three directions. The hexagonal pattern presents three types of cracks each in three possible directions. In addition a given crack can end in front of different elements and each alternative should in principle be considered. Precluding an exhaustive optimization procedure where all the possibilities are tested it was suggested that the designer choose a *trap* element which is designed to arrest the crack and sacrifice other elements along the crack path. It was also shown that a prior study of the cracks can reduce the number of possibilities to a more tractable set. Since engineering judgment is involved the final design is always checked against all possible cracks. The actual computations were performed on a Matlab platform and for the optimization we have used a sequential quadratic optimization algorithm.

Two types of redesigns were considered. In the cell design case material was moved between the, otherwise uniform, elements. In the second design all elements were identical but had variable cross-sections. The parameters controlling the contour of the elements were here the design variables. The computations for the cell design were repeated for small repeating units (three design variables) and for larger ones (twelve design variables). As a rule results indicate that the stretch dominated triangular pattern is much more crack-resistant than the corresponding flexion dominated hexagonal layout. It is also much more sensitive to moving material between uniform elements than to the use of elements with variable thickness. An opposite conclusion can be drawn for the hexagonal honeycomb. A practical conclusion which could be drawn from the present work is that in order to increase the resistance to crack propagation of two dimensional cellular material one should redistribute the material between the elements of the repetitive model when the primary deformation mode of the structural elements is axial

deformation. In the case of models where bending is dominant the use of elements with variable thickness is the way to go. With the methodology presented herein one can quantify the expected improvements in a coherent manner. It is noteworthy that the computations, although confined to the repetitive unit, produce exact results for the infinite model.

The feasibility of manufacturing such optimal cellular materials may, at present, be questionable. It is however difficult to foresee what the future holds in store. MEMS technology, amongst others, could perhaps implement such optimal layouts.

References

- [Bolton 1998] W. Bolton, *Engineering materials technology*, 3rd ed., Butterworth-Heinemann, Oxford, 1998.
- [Chen et al. 1998] J. Y. Chen, Y. Huang, and M. Ortiz, “Fracture analysis of cellular materials: a strain gradient model”, *J. Mech. Phys. Solids* **46**:5 (1998), 789–828.
- [Choi and Sankar 2005] S. Choi and B. V. Sankar, “A micromechanical method to predict the fracture toughness of cellular materials”, *Int. J. Solids Struct.* **42**:5–6 (2005), 1797–1817.
- [Deshpande et al. 2001] V. S. Deshpande, M. F. Ashby, and N. A. Fleck, “Foam topology: bending versus stretching dominated architectures”, *Acta Mater.* **49**:6 (2001), 1035–1040.
- [Fleck and Qiu 2007] N. A. Fleck and X. Qiu, “The damage tolerance of elastic-brittle, two-dimensional isotropic lattices”, *J. Mech. Phys. Solids* **55**:3 (2007), 562–588.
- [Fuchs and Ryvkin 2002] M. B. Fuchs and M. Ryvkin, “Explicit exact analysis of infinite periodic structures under general loading”, *Struct. Multidiscip. O.* **23**:4 (2002), 268–279.
- [Fuchs et al. 2004] M. B. Fuchs, M. Ryvkin, and E. Grosu, “Topological alternatives and structural modeling of infinite grillages on elastic foundations”, *Struct. Multidiscip. O.* **26**:5 (2004), 346–356.
- [Gibson and Ashby 1997] L. J. Gibson and M. F. Ashby, *Cellular solids: structure and properties*, 2nd ed., Cambridge University Press, Cambridge, 1997.
- [Huang and Gibson 1991] J. S. Huang and L. J. Gibson, “Fracture toughness of brittle honeycombs”, *Acta Metall. Mater.* **39**:7 (1991), 1617–1626.
- [Lipperman et al. 2007a] F. Lipperman, M. Ryvkin, and M. B. Fuchs, “Fracture toughness of two-dimensional cellular material with periodic microstructure”, *Int. J. Fract.* **146**:4 (2007), 179–190.
- [Lipperman et al. 2007b] F. Lipperman, M. Ryvkin, and M. B. Fuchs, “Nucleation of cracks in two-dimensional periodic cellular materials”, *Comput. Mech.* **39**:2 (2007), 127–139.
- [Lipperman et al. 2008a] F. Lipperman, M. B. Fuchs, and M. Ryvkin, “Stress localization and strength optimization of frame material with periodic microstructure”, *Comput. Methods Appl. Mech. Eng.* **197**:45–48 (2008), 4016–4026.
- [Lipperman et al. 2008b] F. Lipperman, M. Ryvkin, and M. B. Fuchs, “Crack arresting low-density porous materials with periodic microstructure”, *Int. J. Eng. Sci.* **46**:6 (2008), 572–584.
- [Maiti et al. 1984] S. K. Maiti, M. F. Ashby, and L. J. Gibson, “Fracture toughness of brittle cellular solids”, *Scr. Metall.* **18**:3 (1984), 213–217.
- [Majid et al. 1978] K. I. Majid, M. P. Saka, and T. Celik, “The theorems of structural variation generalized for rigidly jointed frames”, *Proc. Inst. Civ. Eng.* **65**:4 Part 2 (1978), 839–856.
- [Michel et al. 1999] J. C. Michel, H. Moulinec, and P. Suquet, “Effective properties of composite materials with periodic microstructure: a computational approach”, *Comput. Methods Appl. Mech. Eng.* **172**:1–4 (1999), 109–143.
- [Nuller and Ryvkin 1980] B. Nuller and M. Ryvkin, “On boundary value problems for elastic domains of a periodic structure deformed by arbitrary loads”, *Proc. State Hydraulic Inst.* **136** (1980), 49–55. In Russian.
- [Quintana Alonso and Fleck 2007] I. Quintana Alonso and N. A. Fleck, “Damage tolerance of an elastic-brittle diamond-celled honeycomb”, *Scr. Mater.* **56**:8 (2007), 693–696.

- [Ryvkin and Nuller 1997] M. Ryvkin and B. Nuller, “Solution of quasi-periodic fracture problems by the representative cell method”, *Comput. Mech.* **20**:1–2 (1997), 145–149.
- [Ryvkin et al. 1999] M. Ryvkin, M. B. Fuchs, and B. Nuller, “Optimal design of infinite repetitive structures”, *Struct. Multidiscip. O.* **18**:2–3 (1999), 202–209.
- [Schmidt and Fleck 2001] I. Schmidt and N. A. Fleck, “Ductile fracture of two-dimensional cellular structures”, *Int. J. Fract.* **111**:4 (2001), 327–342.
- [Warren and Kraynik 1987] W. E. Warren and A. M. Kraynik, “Foam mechanics: the linear elastic response of two-dimensional spatially periodic cellular materials”, *Mech. Mater.* **6**:1 (1987), 27–37.
- [Warren and Kraynik 1988] W. E. Warren and A. M. Kraynik, “The linear elastic properties of open-cell foams”, *J. Appl. Mech. (ASME)* **55** (1988), 341–346.

Received 5 Mar 2008. Revised 7 Dec 2008. Accepted 14 Jan 2009.

FABIAN LIPPERMAN: fabian@eng.tau.ac.il

School of Mechanical Engineering, Tel Aviv University, Ramat Aviv 69978, Israel

MICHAEL RYVKIN: arikr@eng.tau.ac.il

School of Mechanical Engineering, Tel Aviv University, Ramat Aviv 69978, Israel

<http://www.eng.tau.ac.il/~arikr/>

MOSHE B. FUCHS: fuchs@eng.tau.ac.il

School of Mechanical Engineering, Tel Aviv University, Ramat Aviv 69978, Israel